무중력에서의 비예혼합 메탄-공기 확산화염의 전산
I. 화염온도와 축방향 유속의 분포

박 외 철
부경대학교 안전공학과
(2003. 9. 8. 접수 / 2004. 1. 7. 채택)

Computation of Nonpremixed Methane-Air Diffusion Flames in Microgravity
I. Profiles of Flame Temperature and Axial Velocity

Woe-Chul Park
Department of Safety Engineering, Pukyong National University
(Received September 8, 2003 / Accepted January 7, 2004)

Abstract : The structure of the nonpremixed methane-air counterflow flames in microgravity was investigated by axisymmetric simulation with Fire Dynamics Simulator (FDS) to evaluate the numerical method and to see the effects of strain rate and fuel concentration on the diffusion flame structure in microgravity. Results of FDS for the methane mole fractions, $x_m = 20$, 50, and 80% in the fuel stream, and the global strain rates $a_g = 20$, 50, and $90s^{-1}$ for each methane mole fraction were compared with those of OPPDIF, an one-dimensional flamelet code. There was good agreement in the temperature and axial velocity profiles between the axisymmetric and one-dimensional computations. It was shown that FDS is applicable to the counterflow flames in a wide range of strain rate and fuel concentration by predicting accurately the flame thickness, flame positions and stagnation points.

초 록 : 수치법을 검증하고 변형률과 연료농도가 무중력 확산화염 구조에 미치는 영향을 파악하기 위해, 무중력에서의 비예혼합 메탄-공기 대향류 화염의 구조를 FDS의 축대칭 모사로 조사하였다. 연료 중의 메탄 몰분율 $x_m = 20$, 50, 80%와 각각의 몰분율에서 변형률 $a_g = 20$, 50, $90s^{-1}$의 계산결과를 1차원 화염코드인 OPPDIF의 결과와 비교하였다. 축대칭 모사로 계산한 온도와 축방향 유속의 분포가 1차원 모사 결과와 잘 일치하였다. 화염의 두께와 위치, 정체점을 잘 예측함으로써 FDS를 넓은 범위의 변형률과 연료농도의 대향류 화염에 적용할 수 있음을 확인하였다.
Key Words : methane-air nonpremixed counterflow flame, microgravity, global strain rate, fuel concentration, temperature, axial velocity

Nomenclature

a_g : global strain rate, s^{-1}
x_m : mole fraction of methane in fuel stream
D : inside diameter of duct, 15mm
L : separation distance between two ducts, 15mm
t : duct thickness, 0.5mm
V_A : air velocity at duct exit, m/s
V_F : fuel velocity at duct exit, m/s
ρ_A : density of air, kg/m^3
ρ_F : density of fuel, kg/m^3

1. Introduction

Studies on structure and extinction of hydrocarbon diffusion flames are important in development of fire suppression agents and in fire safety consideration. A simple counterflow flame between two opposed ducts

wcpark@pknu.ac.kr

have been utilized for study on fire suppression agents (e.g., Hamins et al.[1]). In microgravity conditions such as a space platform fire, strain rates are low and no buoyancy effects exist, and the counterflow flames in microgravity are much thicker than those in normal gravity at low strain rates. Among the studies on counterflow flame in microgravity, Maruta et al.[2] investigated the low and moderately strained flames with measurements and computations. The experiments were carried out through drop tests to achieve the microgravity conditions for a short duration. On the other hand, the numerical investigations were performed by using OPPDIF[3], an one-dimensional flamelet code based on a similarity solution by neglecting buoyancy. Since OPPDIF treats the axisymmetric flame as an one-dimensional and steady flow problem, it provides information on flame structure of the flame limited along the centerline of the ducts and in microgravity only.

The NIST Fire Dynamics Simulator (FDS)[4] was developed for unsteady three-dimensional large-scale fire phenomena with a large eddy simulation. FDS also employs the direct numerical simulations for small-scale problems like the counterflow flames, computing directly transport and dissipative process. Park[5] showed that the direct numerical simulations in FDS is applicable to the buoyancy dominated low strain rate non-premixed counterflow flames in normal gravity. An extinction of a fire, however, is not predictable with FDS since it employed a mixture fraction combustion formulation. In spite of such a shortcoming, if FDS is proved to be accurate in prediction of flame structure, it will be very useful providing much more information and physical insights on the diffusion flames, compared with OPPDIF. FDS solves the unsteady problems in three-dimensional situations and in normal and zero gravity or transition from normal to zero gravity, while OPPDIF does the steady one-dimensional combustion problems in zero gravity conditions.

Although FDS have been utilized to the counterflow flames by Park[5], and Park and Hamins[6], further investigations are needed in a wide range of fuel concentrations and global strain rates. The objectives of this study are to evaluate FDS for the counterflow flames at various global strain rates and methane concentrations, and to investigate the effects of the strain rate and fuel concentration on the flame structure in microgravity. Comparisons were made between the results of FDS and those of OPPDIF. The effects of on the flame thickness and radius were also investigated. The profiles of temperature and axial velocity along the duct centerline are presented in Part I, and the flame thickness and radius as functions of strain rate and fuel concentration are presented in Part II.

2. Methodology

The counterflow burner has two opposed circular ducts separated by a distance L as shown in Fig. 1. A mixture of methane and agent(nitrogen) is supplied through the lower fuel duct, and air flows in the oxidizer duct. D is the inside diameter of duct, t is the thickness of duct wall. The oxidizer is pure air, and the fuel is composed of a mixture of methane and nitrogen. The dimensions and the numerical parameters to be investigated are listed in Table 1.

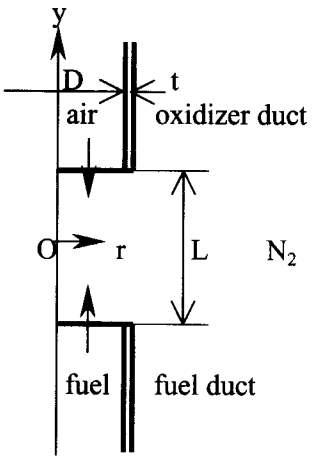

Fig. 1. Schematic of the counterflow burner

Table 1. Dimensions of burner and numerical parameters

D (mm)	15
t (mm)	0.5
L (mm)	15
x_m (%)	20, 50, 80
a_e (s^{-1})	20, 60, 90

The top hat velocity profile was imposed at the both duct exits, and no slip condition on the duct walls. The velocity boundary conditions at the duct exits were investigated by Park and Hamins[6]. The temperature of the fuel and air streams was set to 25°C. In FDS, the gravity was set to zero, and radiation loss was not included in both FDS and OPPDIF since it is small at low strain rates[2].

For a given global strain rate ag and fuel concentration xm, VA and VF are calculated by the definition of the global strain rate,

$$a_g = -\frac{2V_A}{L}\left[1-\frac{V_F}{V_A}\left(\frac{\rho_F}{\rho_A}\right)^{0.5}\right] \quad (1)$$

where, $V_A = -V_F$, ρ_A is the density of air, and ρ_F is the density of the methane and nitrogen mixture at 1 atm and 25°C.

Following the previous study of Park[5], the computational domain was taken to be 40mm×40mm in both the r- and y- directions, and the grid spacing was taken to be 0.5mm uniformly. Since a steady state flame was obtained in about 0.7s, computations were carried out up to 1.0 s, and the average temperature and axial velocity along the center line (y-axis) were calculated from the instantaneous values of 0.8~1.0s.

The solution procedures are described in detail in McGrattan et al.[4] and Park and Hamines[6].

3. Results and Discussion

3.1. x_m = 20%

Fig. 2 compares the flames simulated by FDS at strain rate a_g = 20, 60 and 90s^{-1} for the methane mole fraction x_m = 20% in the fuel stream, that is, fuel of 20% CH_4 + 80% N_2. Changes in the thickness and radius of the flames, of which definitions and quantitative results are to be discussed in Part II, are discernible: The flame thickness decreases and the flame radius increases with increasing strain rate. In Eq. (1), the axial velocities in the fuel and oxidizer streams are proportional to the strain rate, and this results in the increase of the flame radius and decrease of the flame thickness. Note that both velocities of the oxidizer stream and the fuel stream are the same for the given fuel concentration in the present study, and that OPPDIF does not provide flame shape since it is not capable of axisymmetric simulations.

In Fig. 3, the profiles of temperature and axial velocity along the duct centerline (y-axis in Fig. 1), at a_g = 20, 60 and 90 s^{-1} for the fuel composed of 20% methane and 80% nitrogen (x_m = 20%) are compared.

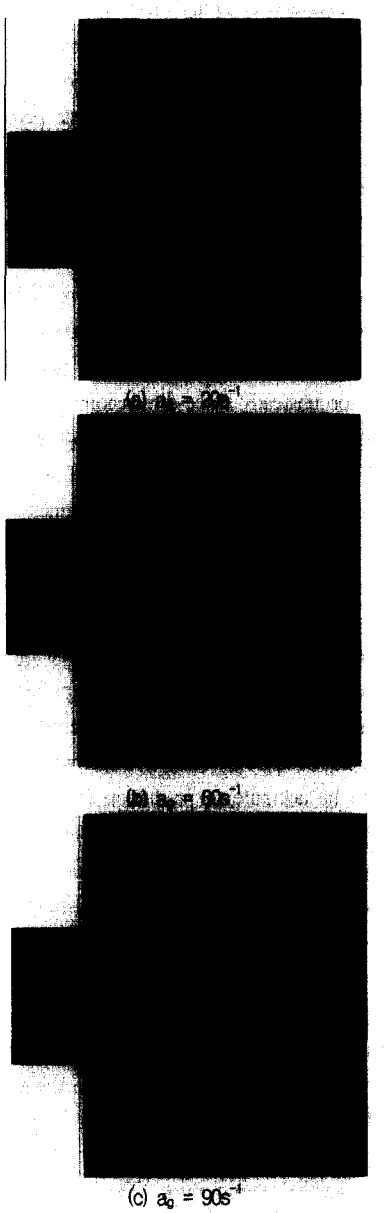

(c) a_g = 90s^{-1}

Fig. 2. Flames for x_m = 20% (FDS)

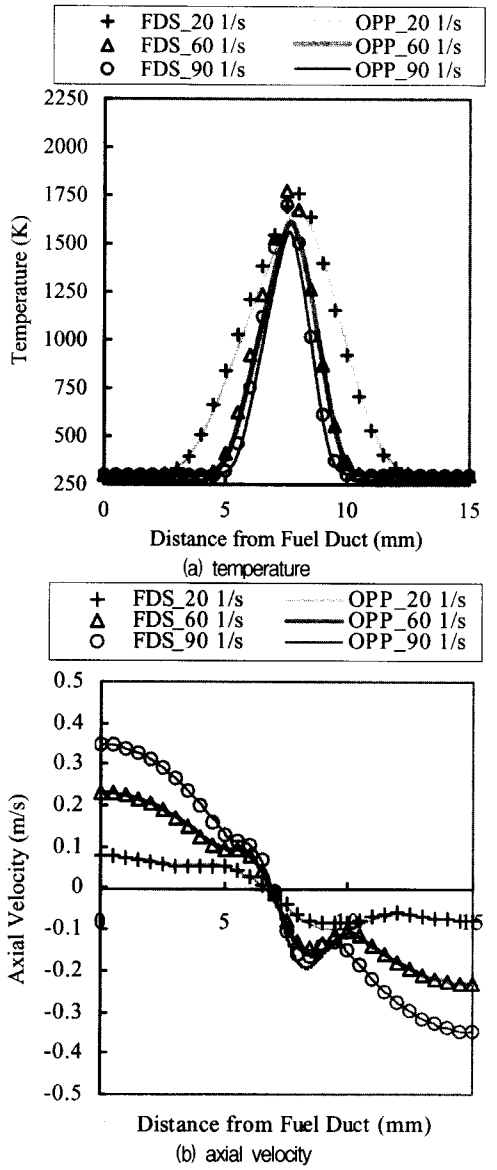

Fig. 3. Comparison of temperature and axial velocity profiles for global strain rates (x_m = 20%)

Both the temperature and axial velocity predicted by FDS are in excellent agreement with those obtained by OPPDIF in this near-extinction fuel concentration case except for the peak flame temperature at a_g = 90s^{-1}. The temperature profiles show more clearly than the flames in Fig. 2 that the flame thickness decreases as the strain rate increases from 20s^{-1} to 60 and 90s^{-1}. The temperature profiles also show the flame is located near the mid-plane between the lower fuel duct and the upper oxidizer duct. The flame position remains unchanged despite of different strain rates at the near-extinction fuel concentration. It is also noted that the stagnation point, where the axial velocity is zero, also remains the same.

3.2. x_m = 50%

The flames obtained with the axisymmetric simulation for moderate fuel concentration, x_m = 50%, are

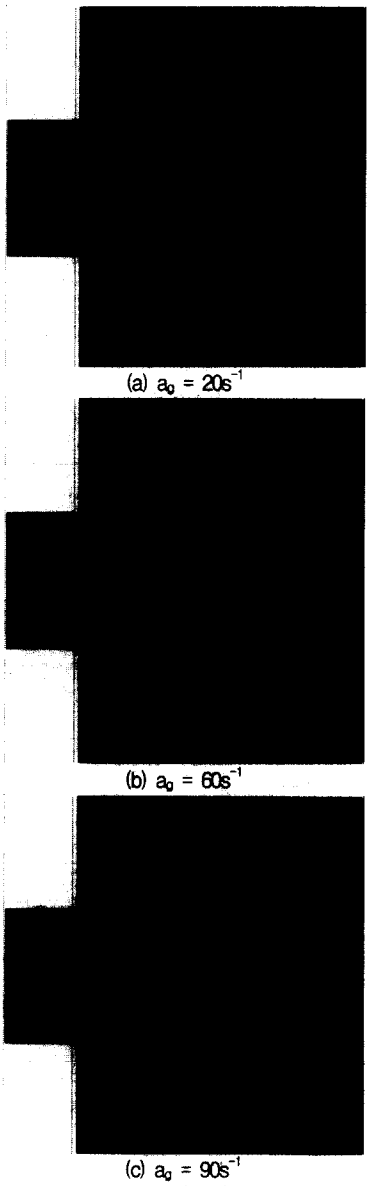

Fig. 4. Flames for x_m = 50% (FDS)

compared in Fig. 4. Similarly to the case of the fuel concentration x_m = 20%, the flame thickness decreases and the flame radius increases as the strain rate increases from 20 to 60 and to 90s^{-1}. Meanwhile Figs. 2a and 4a show that the flame of x_m = 50% at the duct centerline is thicker than that of the lower fuel concentration, x_m = 20%.

The corresponding temperature and axial velocity along the duct centerline at a_g = 20, 60 and 90s^{-1} of the axisymmetric computations (FDS) are compared with those of one-dimensional computations (OPPDIF) in Fig. 5. Discrepancies in the axial velocity in the high temperature region at a_g = 90s^{-1} and the peak flame temperatures between the two different methods are observed. Except that the both numerical methods are in good

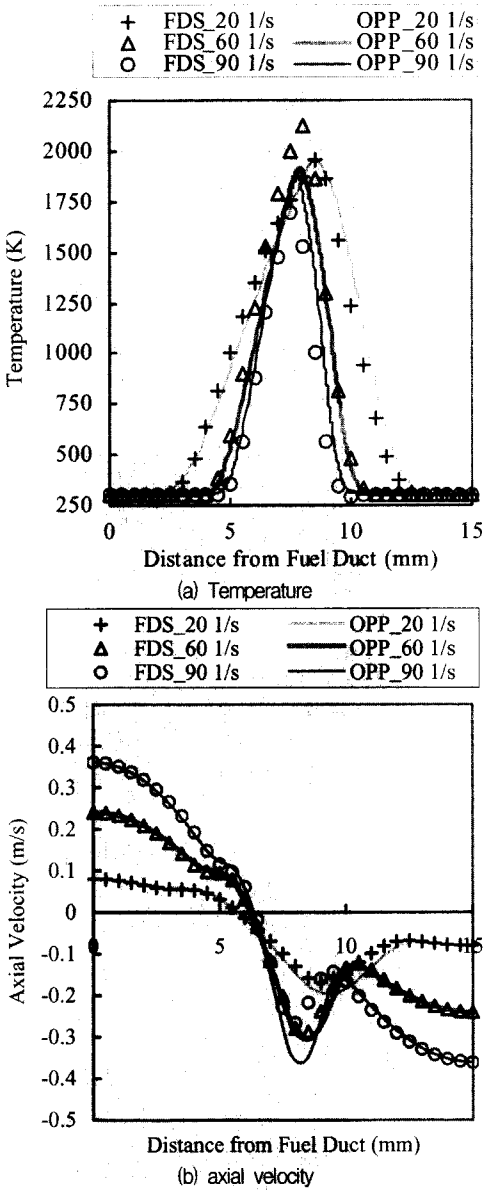

Fig. 5. Comparison of temperature and axial velocity profiles for global strain rates (x_m = 50%)

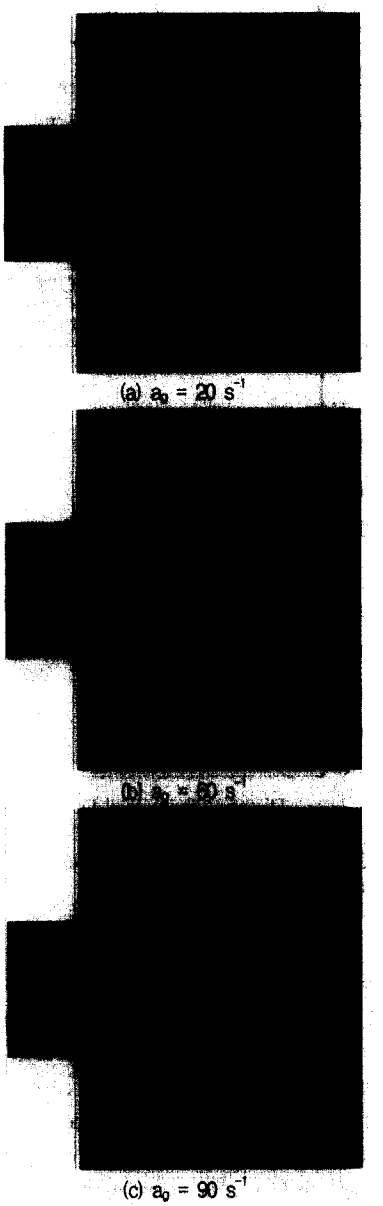

Fig. 6. Flames at x_m = 80% (FDS)

agreement. Decreases in flame thickness with increasing strain rate and the flame positions predicted by the axisymmetric computations agree very well with those obtained by the one-dimensional computations as seen in the fuel lean case of x_m = 20%. The flame positions near the mid-plane between the two ducts at a_g = 20 and 60s^{-1}, while it is shifted towards the upper oxidizer duct a_g = 90s^{-1}. The flame positions, flame thickness and the stagnation points for the three different strain rates are in good agreement between FDS and OPPDIF.

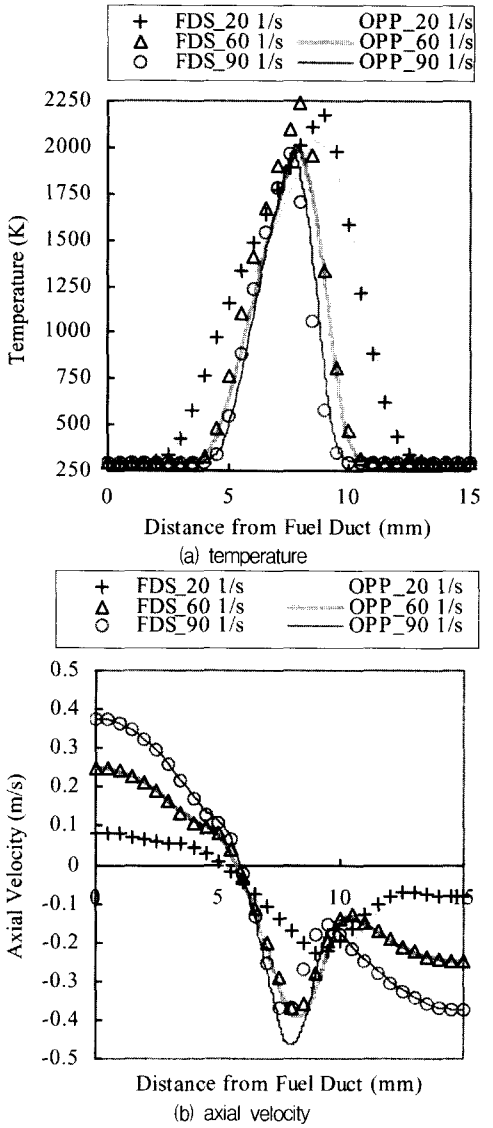

Fig. 7. Comparison of temperature and axial velocity profiles for global strain rates (x_m = 80%)

3.3. x_m = 80%

Fig. 6 shows the flames of the three strain rates, a_g = 20, 60 and 90s^{-1}, in the fuel rich case, x_m = 80%, i.e., 80% methane and 20% nitrogen in the fuel stream. Compared with the lower fuel concentrations x_m = 20 and 50%, the flame thickness is increased with the fuel concentration.

Fig. 7 compares the corresponding temperature and axial velocity profiles along the y-axis. Results are very similar to the cases of the fuel lean (x_m = 80%,) and moderate fuel concentrations (x_m = 50%). Although there exists the similar discrepancy in the axial velocity to the cases of the lower fuel concentrations, the temperature and axial velocity profiles of the two methods are in good agreement. The flame positions and stagnation points between the two numerical methods also agree well.

4. Conclusions

The nitrogen diluted methane-air diffusion flames in microgravity was computed by axisymmetric simulation with Fire Dynamics Simulator to evaluate the numerical method and to investigate the effects of strain rate and fuel concentration on the diffusion flame structure in microgravity. Results were compared with those of OPPDIF, an one dimensional flamelet code. The mole fraction of methane, x_m = 20, 50 and 80% in the fuel stream, and the global strain rates a_g = 20, 50, 90s^{-1} were chosen as numerical parameters. There was good agreement in the temperature and axial velocity profiles between the axisymmetric and one-dimensional computations except for the axial velocity in the high temperature region at the high strain rate and the peak flame temperature. The flame thickness, flame positions and stagnation points were also in good agreement. It was shown that the flame thickness decreases and flame radius increases with increasing strain rate and decreasing fuel concentration.

Acknowledgement

The author is grateful to Dr. Anthony Hamins and Dr. Kevin McGrattan at National Institute of Standards

and Technology for helpful discussions.

References

1) A. Hamins, D. Trees, K. Seshadri and H.K. Chelliah, "Extinction of Nonpremixed Flames with Halogenated Fire Suppressants", Combustion and Flames, Vol. 99, pp. 221~230, 1994.
2) K. Maruta, M. Yoshida, H. Guo, Y. Ju and T. Niioka, "Extinction of Low-Streched Diffusion Flame in Microgravity", Combustion and Flames, Vol. 112, pp. 181~187, 1998.
3) A. Lutz, R.J. Kee, J. Grcar and F.M. Rupley, "A Fortran Program Computing Opposed Flow Diffusion Flames", SAND96-8243, Sandia National Laboratories, Livermore, CA, U.S.A., 1997.
4) K.B. McGrattan, H.R. Baum, R.G. Rehm, A. Hamins, G.P. Forney, J.E. Floyd and S. Hostikka, Fire Dynamics Simulator Technical Reference Guide, v.3, National Institute of Standards and Technology, Gaithersburg, MD, U.S.A., 2002.
5) W.C. Park, "An Evaluation of a Direct Numerical Simulation for Counterflow Diffusion Flames", J. Korea Institute for Industrial Safety, Vol. 16, No. 4, pp. 74~81, 2001.
6) W.C. Park and A. Hamins, "Investigation of Velocity Boundary Conditions in Counterflow Flames", KSME Int'l J., Vol. 16, pp. 262~269, 2002.